Article:
Mao, X and Jaworski, AJ (2010) Oscillatory flow at the end of parallel-plate stacks: Phenomenological and similarity analysis. Fluid Dynamics Research, 42 (5). 5. 055504 - 055504. ISSN 0169-5983

https://doi.org/10.1088/0169-5983/42/5/055504

Oscillatory flow at the end of parallel plate stacks – phenomenological and similarity analysis

Xiaoan MAO and Artur J. JAWORSKI [1]

School of Mechanical, Aerospace and Civil Engineering, The University of Manchester,
George Begg Building, Sackville Street, Manchester, M13 9PL, UK

Abstract: This paper addresses the physics of the oscillatory flow in the vicinity of a series of parallel plates forming geometrically identical channels. This type of flow is particularly relevant to thermoacoustic engines and refrigerators, where a reciprocating flow is responsible for the desirable energy transfer, but it is also of interest to general fluid mechanics of oscillatory flows past bluff bodies. In this paper the physics of an acoustically induced flow past a series of plates in an isothermal condition is studied in detail using the data provided by PIV imaging. Particular attention is given to the analysis of the wake flow during the ejection part of the flow cycle, where either closed re-circulating vortices or alternating vortex shedding can be observed. This is followed by a similarity analysis of the governing Navier-Stokes equations in order to derive the similarity criteria governing the wake flow behaviour. To this end, similarity numbers including two types of Reynolds number, Keulegan-Carpenter number and a non-dimensional stack configuration parameter, d/h are considered and their influence on the phenomena discussed.

1. Introduction and background

In thermoacoustic devices, an acoustic wave interacts with internal solid structures (referred to as thermoacoustic stacks or regenerators) either to produce acoustic power, induced by a temperature gradient on the stack (an engine), or to obtain a temperature gradient along the stack, induced by an imposed acoustic wave (a cooler). This is based on the well-known thermoacoustic effect (Rayleigh, 1894), where appropriately phased pressure and velocity oscillations enable the compressible fluid to undergo a thermodynamic cycle in the vicinity of a solid body. Figure 1 shows schematically the physics behind generating useful acoustic energy in a standing wave thermoacoustic engine. Detailed analysis is provided by Swift (1988).

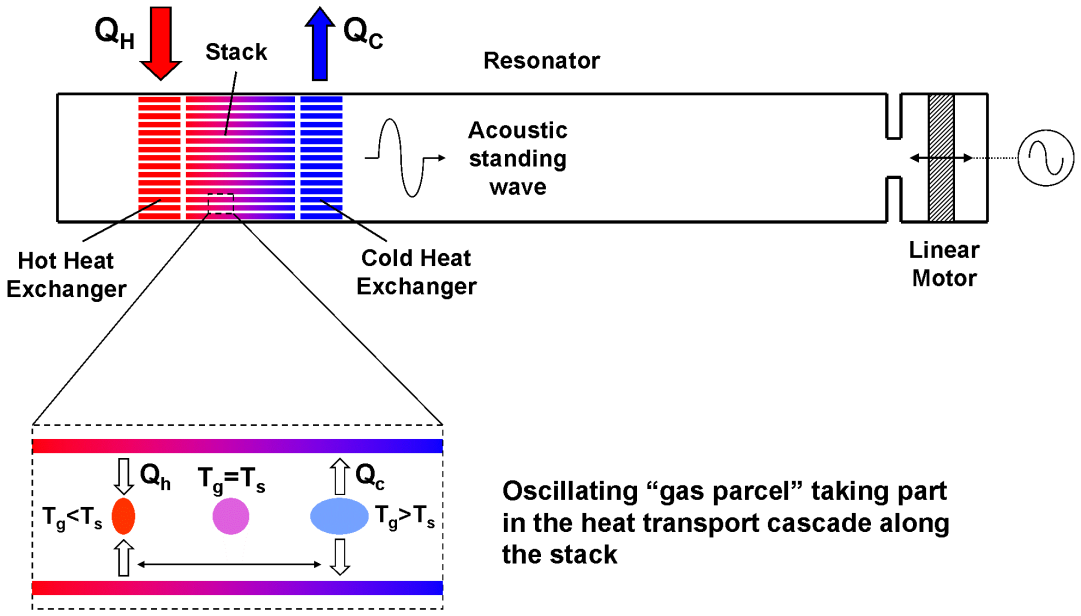

Figure 1 Illustration of the oscillatory gas motion coupled with heat transfer to/from the solid.

[1] Corresponding author: T: +44(0)161 275 4352, F: +44(0)161 306 3755, E-mail: a.jaworski@manchester.ac.uk

The main advantages of thermoacoustic devices are their simplicity of construction, high reliability, potentially low cost and environmental friendliness. The thermodynamic cycle takes place in an environmentally benign oscillating gas (air, helium, nitrogen etc) without the need for any timing mechanisms involving moving parts. Thermoacoustic devices are an attractive alternative in certain niche applications including electricity generation for spacecraft, low cost electricity generators for rural areas, gas liquefaction systems for remote oil rigs, or for utilisation of industrial waste heat. However, systems built so far suffer from a poor thermodynamic efficiency compared to the efficiency that is theoretically achievable (Paek et al., 2005). It is thought that a better understanding of the thermo-fluid processes within the internal components is important to aid the design of thermoacoustic systems of higher efficiency.

It is well known that linear thermoacoustic theory can reliably predict the performance at low amplitudes of acoustic pressure (Rott, 1980; Swift, 1988). However at high amplitudes, which are required for such system to operate in practical industrial applications, nonlinear effects become significant; these include acoustic streaming as well as vortex shedding and turbulence generation, especially at abrupt changes of cross-sectional areas such as the end of thermoacoustic stacks. Therefore there is a need for understanding the oscillatory flow processes in the vicinity of such internal structures, which potentially can adversely affect the achievable efficiencies of thermoacoustic systems.

In thermoacoustic devices, arrays of tightly spaced parallel plates are often used as stacks or regenerators because of the ease of manufacture and their theoretical performance (Backhaus and Swift, 2001). Similarly, some of the popular thermoacoustic heat exchangers (fin-and-tube type) are essentially parallel-plate structures that facilitate heat input and removal to and from stack/regenerator assemblies. Clearly, the heat transfer efficiencies achieved by thermoacoustic heat exchangers are strongly affected by the state of the flow passing through. In the general sense, flows past these types of internal structures can be seen as a problem of an oscillatory flow with zero mean past a series of bluff bodies (i.e. individual plates or fins), which is the background of present paper.

Over the last century, numerous studies of the flow field behaviour due to steady flows past bluff bodies have been conducted, one of the earliest usually cited being work of von Karman on vortex shedding behind a circular cylinder (Kovasznay, 1949). However a somewhat more relevant topic to the current work is the oscillatory flow past bluff bodies. Majority of such studies have been conducted for circular cylinders due to the practical applications of wind engineering, marine and coastal engineering, chemical engineering and heat exchangers – good examples are given by Berger and Wille (1972), Bearman et al. (1980) and Bearman (1984).

The oscillatory flow around stacks of plates of finite thickness and square edges has received some attention both numerically (Worlikar et al., 1996, Worlikar and Knio, 1996) and experimentally, for example by Mao et al. (2005), Mao et al. (2008), Aben et al. (2009) and most recently Shi at al. (2009). Some important flow features such as symmetrical concentrated vortex pairs attached to the plate ends or the elongated vortex pairs which break up into "vortex-street" type of structures were observed (Mao et al., 2008). In various experimental papers of this kind the stack plates used have a relatively large range of thickness: from 0.15 mm to a few millimetres and as a result, the flow behaviour at the stack end differs dramatically from one case to another. For example, as reported by Mao et al. (2008), flow features at the end of a 5.0 mm thick stack plates resemble von Karman vortex shedding, while, in nearly the same conditions, flow features at the end of 1.1 mm thick plates include long shear layers that lose their stability and break up into discrete vortices. However, the purpose of the work by Mao et al. (2008) was to study the development of the flow structures (patterns), formed around the stack end during the oscillation cycle, as a function of the flow oscillation amplitude (described by the drive ratio) varying within a certain range. Thus the flow behaviour was essentially studied as a function of the "phase Reynolds number", as well as the "peak Reynolds number". In the statement of future work, it was noted that a more comprehensive similarity analysis should be carried out in future and it has been hypothesised that the appropriate similarity numbers such as Reynolds number, Keulegan-Carpenter number (KC) and a geometrical parameter such as for example stack porosity could be used for characterization of the oscillatory flow past parallel plate stacks.

In practical thermoacoustic devices the plate thickness is often of the order of 0.1 mm, while heat exchanger fins can be significantly thicker, e.g. in the range of 2.0 mm to ensure good heat removal properties – e.g. see Hofler (1986) or Backhaus and Swift (2001). Therefore it is practically important to understand the flow behaviour at the stack end for a

wide range of stack geometries, the controlling parameters and their critical values to distinguish the different flow regimes. Current work explores further the ideas put forward in the previous work by Mao at al. (2008) in order to study the similarity of the oscillating flow around parallel-plate stacks, and attempt to map the flow conditions in a non-dimensional parameter space. In this paper, the common features of the oscillatory flow at the stack end are presented first, based on the PIV measurements of velocity and vorticity fields near parallel-plate stacks in an isothermal condition (i.e. neglecting heat transfer effects). Then a set of non-dimensional parameters is proposed by normalising the governing Navier-Stokes equations to describe the oscillatory flow around an array of rectangular plates, followed by further analysis and discussion.

2. Experimental apparatus and method

The experimental apparatus used in the current study has been described in detail by Marx et al. (2006) while the details of the Particle Image Velocimetry (PIV) measurement system implemented within the rig were given by Mao et al. (2008). Therefore only the essential information will be repeated in this paper. As illustrated in Figure 2, the rig is essentially a standing wave resonator made out of transparent duct with 136 mm × 136 mm cross section, operating at 13.1 Hz, and filled with air at atmospheric conditions. Within the resonator, two different stacks of plates (1.1 and 5.0 mm thick plates with spacing between plates of 5.0 and 10.0 mm, respectively) were subjected to acoustic excitation, which in turn creates oscillatory flow conditions in the vicinity of the stack. Several levels of acoustic excitation, expressed in terms of the so-called drive ratio, D_r , the ratio of the maximum acoustic pressure amplitude (as indicated by the microphone shown in Figure 2) to the mean pressure, were used for each stack configuration. In this way the dependence of the flow characteristics on the displacement and velocity amplitudes of the oscillatory flow could be studied.

The oscillatory flow at the stack end, in the plane perpendicular to the stack plates but along the resonator axis, was recorded using the phase-locked PIV measurement. 20 phases in each acoustic cycle (every 18 degrees) were investigated. For each phase, 100 instantaneous velocity fields were obtained and the ensemble-averaged (mean) velocity fields were further used to obtain the vorticity fields, Ω, used in subsequent figures.

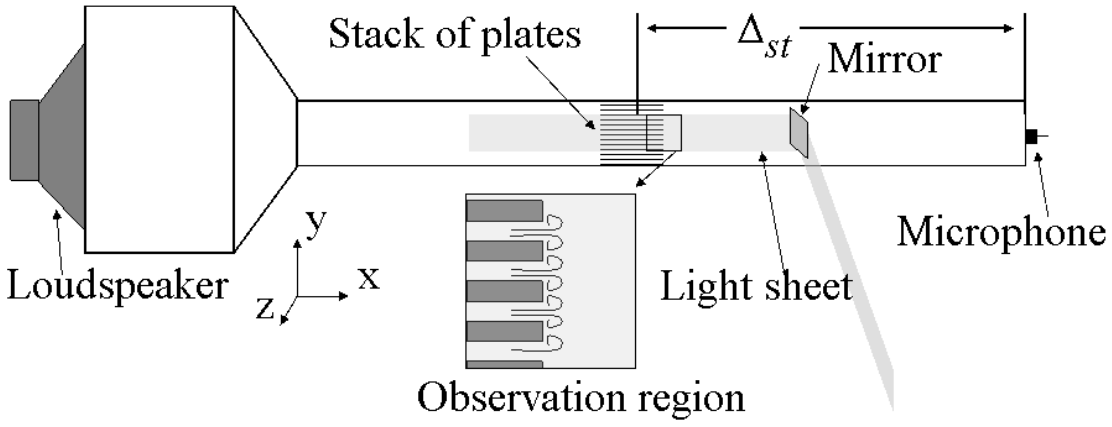

Figure 2 Schematic illustration of the experimental rig.

3. Physics of the oscillatory flow: linear theory versus experimental observations

3.1. Linear theory approximation

When the flow inside a channel formed by parallel plates is not affected by the "entrance effect" caused by the discontinuity of the solid boundary condition at the plate end, and the amplitude of the flow oscillation is sufficiently small for the flow to remain laminar, the profile of the longitudinal velocity component, u, across the channel can be well described by the following equation written in complex notation (Arnott 1991, Swift 2001):

$$u_1(x,y,t) = \frac{p_A \sin(kx)}{\phi \rho c}\left[1 - \frac{\cosh[(1+i)y/\delta_\nu]}{\cosh[(1+i)y_0/\delta_\nu]}\right]e^{i\omega t} \quad (1)$$

with the continuity of the volume flow rate considered in the stack. Subscript '1' indicates that the velocity is an acoustic variable that has the frequency of the acoustic oscillation; the peak acoustic pressure amplitude, p_A, is measured at the nearest pressure antinode; x is the location of the stack in the resonator relative to the pressure antinode, and ϕ is the porosity of the stack, defined as the ratio of the void cross sectional area of the stack to its total area; y is the distance from the centreline of the channel of width of $2y_0$, and $\delta_\nu = (2\nu/\omega)^{1/2}$ is the viscous penetration depth, $\nu = \mu/\rho$ being the kinematic viscosity; c is the speed of sound. It can be seen that the time dependent velocity is defined by the product of three terms. The first term: $p_A \sin(kx)/\phi\rho c$, which can also be denoted by $\langle u_{1,x} \rangle$, is defined as an amplitude of the cross-sectional average velocity (over y) of the flow in the stack. It can be calculated from the linear acoustic field in a resonator, as if the stack was absent, however the porosity in the denominator provides the correct scaling to account for the stack presence. $e^{i\omega t} = \cos(\omega t) + i\sin(\omega t)$ indicates the time dependence of the velocity. The term in the square bracket defines the spatial distribution of the velocity in the parallel channels formed by the plates, introduced by the viscous effects.

The viscous effects are normally limited to a thin boundary layer close to the plate surface. In the flow channels formed between parallel plates, this boundary layer limit is approached at about five times δ_ν from the solid body. Therefore, for a flow channel with $2y_0 > 10\delta_\nu$, the flow in the central region of the channel is practically unaffected by the boundary conditions, which means that the velocity profiles are relatively flat in the central region. In this case, the presence of neighbouring plates has negligible effects on the velocity profiles around the plate under consideration, except that it does change the average velocity amplitude in the stack of plates due to the reduction of the cross-sectional area (compared to an empty resonator).

It should also be noted that in the boundary layer the velocity profiles often exhibit an "annular effect" which is a common feature of oscillatory flows: with the increasing distance from the wall, the velocity values often increase to reach a local maximum, before they decrease further away from the wall. This name follows the terminology first introduced in studies of the oscillatory flow in pipes, where it was more appropriate. The "annular effect" essentially promotes a double shear layer structure on each side of the plate. The "inner" shear layer (closer to the plate surface), however, seems always dominant because of the larger strain, while the shear layer further away from the plate surface is weaker, although still discernible. The "inner" shear layer is essentially limited to a region of about $2\delta_\nu$ from the plate surface.

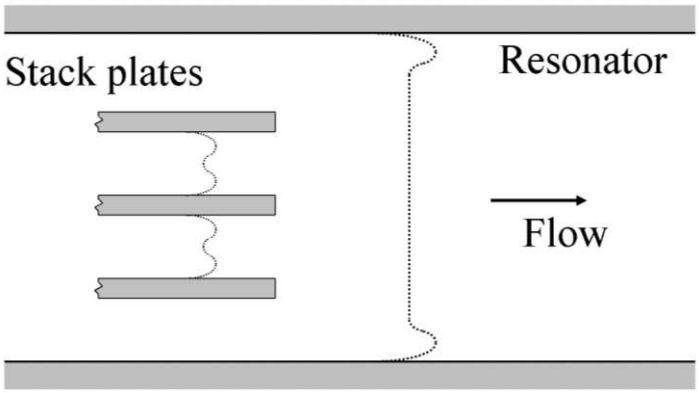

Figure 3 Schematic of velocity profiles in the resonator and inside the stack channels, in the half cycle when the flow direction is from left to right. Only parts of three plates are shown.

Figure 3 shows schematically the velocity profiles in two locations when the flow is generally from left to right: one inside the stack and the other outside the stack, both being sufficiently far away from the stack end not to be affected by one another. In the stack channel the velocity profile affected by the viscous effects extends from the plate surface.

Within the resonator the viscous effects are only limited to a relatively short distance from the resonator wall – the flow in most of the cross sectional area of the resonator behaves as an inviscid plug flow with a flat velocity profile.

3.2. Experimental observations at the end of stack

Of course, in practical systems the description provided by the linear theory is invalid close to the abrupt changes in the resonator cross section, where the velocity profiles need to "adjust" themselves to the discontinuities. Figure 4 is a representative illustration of the velocity field (black arrows), superimposed on the vorticity field (colour contours) related to the flow induced at the end of 1.1 mm thick plate at D_r = 0.3% for phases Φ1 to Φ8. The arrows on the streamlines indicate the flow in this part of the acoustic cycle is from left to right. The position of each phase in the acoustic cycle is represented on the plot of acoustic velocity versus time in the right bottom corner of Figure 4.

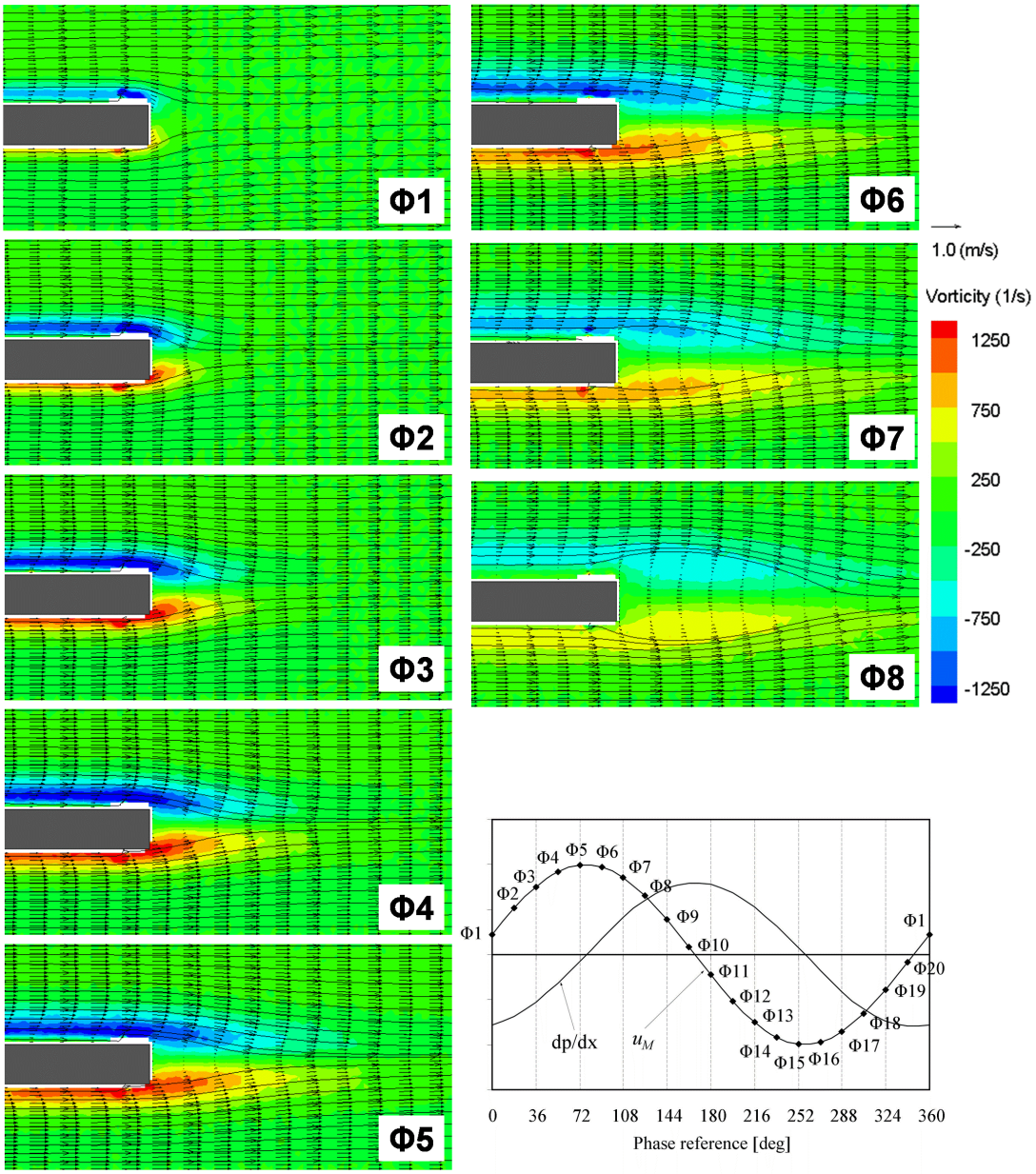

Figure 4 Mean velocity field (black arrows) superimposed on vorticity field (colour contour) in phases Φ1 to Φ8, for Dr = 0.3%. The streamlines indicate the flow is from left to right. Plate thickness is 1.1mm and plate spacing is 5.0 mm. The positions of the phases corresponding to the acoustic cycle are shown in the bottom right corner.

Close to the end of the sharp-edged plate, the flow separation occurs at the trailing edges, during the phases when the flow is out of the stack into the open area of the resonator. When the amplitude of the flow velocity oscillation is small,

a distinct symmetric closed near-wake (i.e. a recirculation region) is formed, as illustrated by the streamlines in Figure 4. This flow field around the stack end could be divided into several characteristic regions as schematically shown in Figure 5, based on the observation of the results of measurements. The shear layers originating from the stack channel extend downstream and join each other forming a shear layer wake. At a position nearest to the plate end, the shear layers meet at the end of the near-wake at a confluence point, where the longitudinal velocity component is zero.

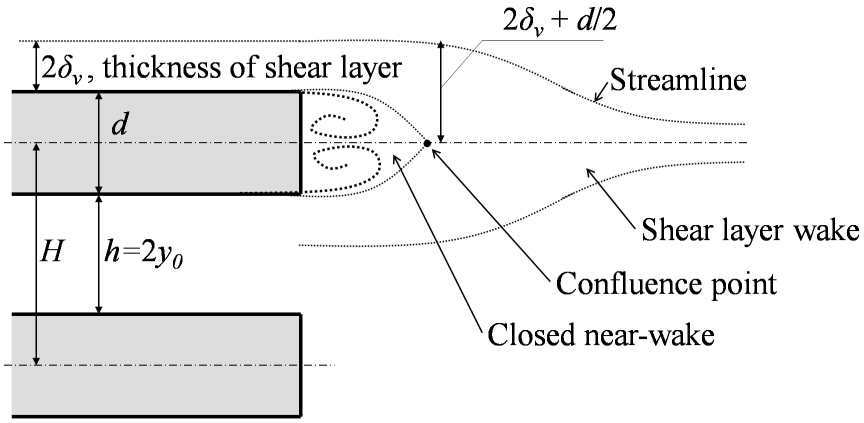

Figure 5 Structure of the flow at the end of a stack of sharp-edged plates of finite thickness.

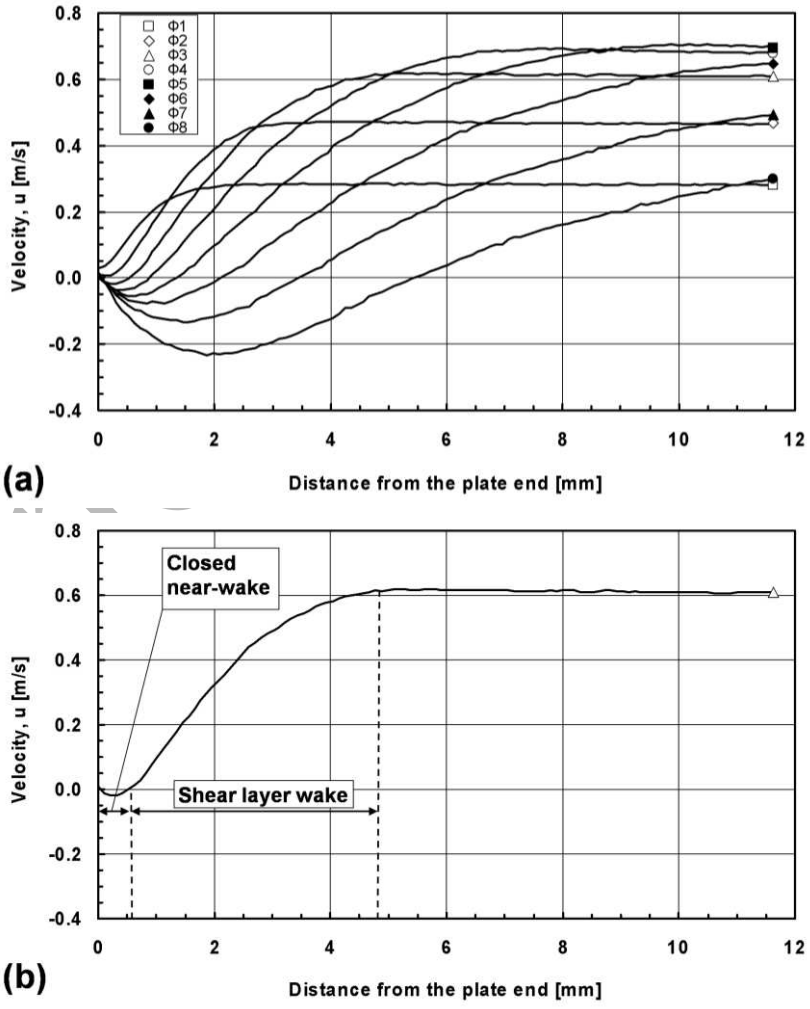

Figure 6 Distribution of the longitudinal velocity, u, along the plate centreline for eight phases (a); Illustration of the regions in the wake (b); Data for stack with d = 1.1 mm and h = 5.0 mm, at Dr = 0.3%.

The closed near-wake normally consists of two counter-rotating eddies, whose lateral distance is normally limited by the plate thickness. The longitudinal size of the closed near-wake, from the plate end to the confluence point, can be estimated from the velocity distribution along the centreline of the stack plate. The velocity profiles along the plate centreline are shown in Figure 6a for phases between Φ1 and Φ8. From phase Φ1 to Φ5, the flow in the stack channel and the "free-stream" outside of the stack is in an acceleration stage and the velocity of the flow increases monotonically with the distance from the plate end, except for the closed near-wake. In phase Φ1, the flow velocity at about 2.2 mm downstream from the plate end is about 0.28 m/s and it is constant further downstream for there is little effect from the flow separation at the plate end. At this phase, the closed near-wake around the plate end is not formed yet, because there is no reversing flow of a negative velocity. In phases from Φ2 to Φ5, the velocity of the flow outside the stack increases. The closed near-wake gradually forms and extends further downstream; at the same time a reversing flow begins to appear.

From phase Φ6, the flow starts to decelerate (due to the decreasing mean flow velocity), while the direction of the flow remains from left to right. It is interesting to see that the closed near-wake continues to extend and this can also be clearly observed in Φ6 – Φ8 in Figure 4, judging from the size of the vortex structure. The maximum velocity of the re-circulating flow is comparable to that of the "free stream" in the deceleration phase Φ7 and Φ8. The confluence point is located where the velocity is zero as illustrated by Figure 6b. It is about 0.55 mm away from the plate end in phase Φ3, i.e. about half of the plate thickness. The shear layer wake region extends from the confluence point to the location where the longitudinal velocity on the plate centreline is comparable to "free stream"; in the example shown in Figure 6b – about 4 times the plate thickness. By looking at phases from Φ1 to Φ4, it is clear that the size of the shear layer wake also increases with time (see the vorticity contour in Figure 4). It is uncertain from this plot, however, whether the development of the shear layer wake would continue in the decelerating stage.

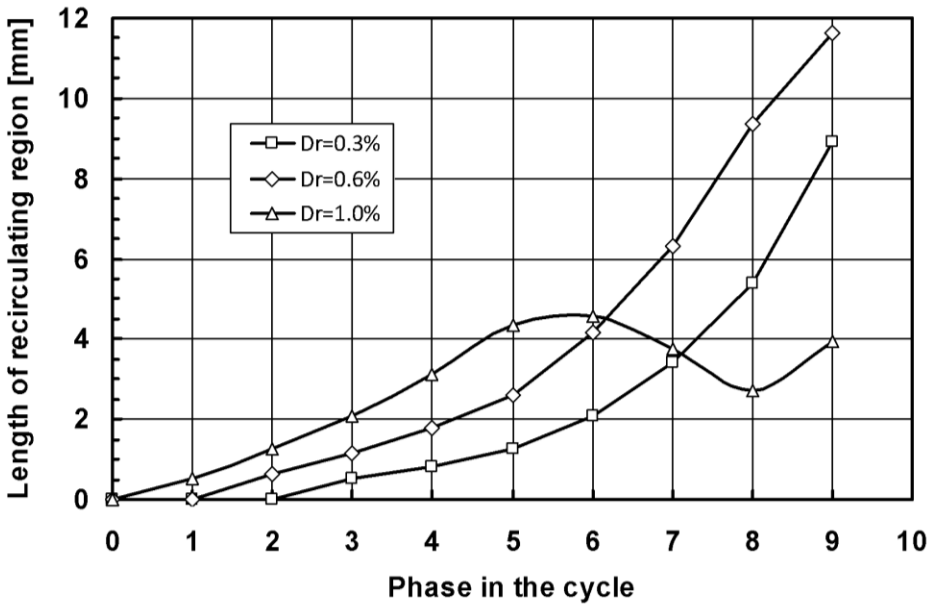

Figure 7 Variation of recirculation region length with consecutive phases in an acoustic cycle, for stack of plates of 1.1 mm thickness.

The longitudinal size of the closed near-wake (the recirculation region) versus the phase in the acoustic cycle is plotted for $D_r = 0.3\%$ in Figure 7, together with analogous plots for $D_r = 0.6\%$, when the shear layer wake remains symmetrical, and $D_r = 1.0\%$ when the shear layers eventually break up and form a sequence of vortices in the wake. For drive ratios 0.3% and 0.6%, the length of the recirculation region increases monotonically with time, the growth being faster for higher drive ratios. However, this behaviour changes for $D_r = 1.0\%$ after phase Φ5. The increase of the recirculation region length is interrupted by the instability of the shear layer wake, as seen in Figure 8. The wake made up of a pair of free shear layers is no longer symmetrical after phase Φ4, but becomes unstable and a lateral oscillation commences at the confluence point, as illustrated by the decrease of the recirculation region length in Figure 7.

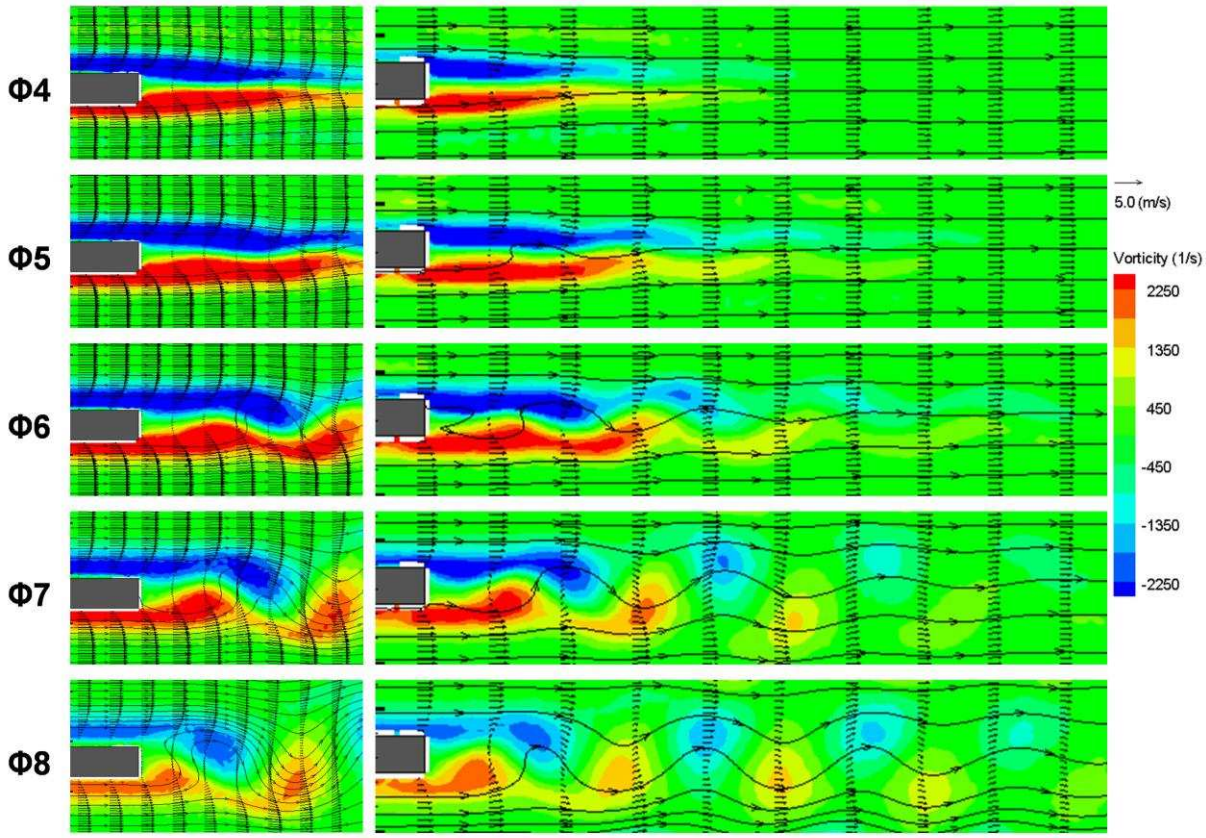

Figure 8 Mean velocity field (black arrows) superimposed on the vorticity field (colour contours) for phases from Φ4 to Φ8 at D_r = 1.0%. The streamlines indicate the flow is from left to right. Stack plates are 1.1 mm thick with 5.0 mm gap between plates. Results in the left column are obtained with a higher spatial resolution, while the right column has a lower spatial resolution but a larger investigated area.

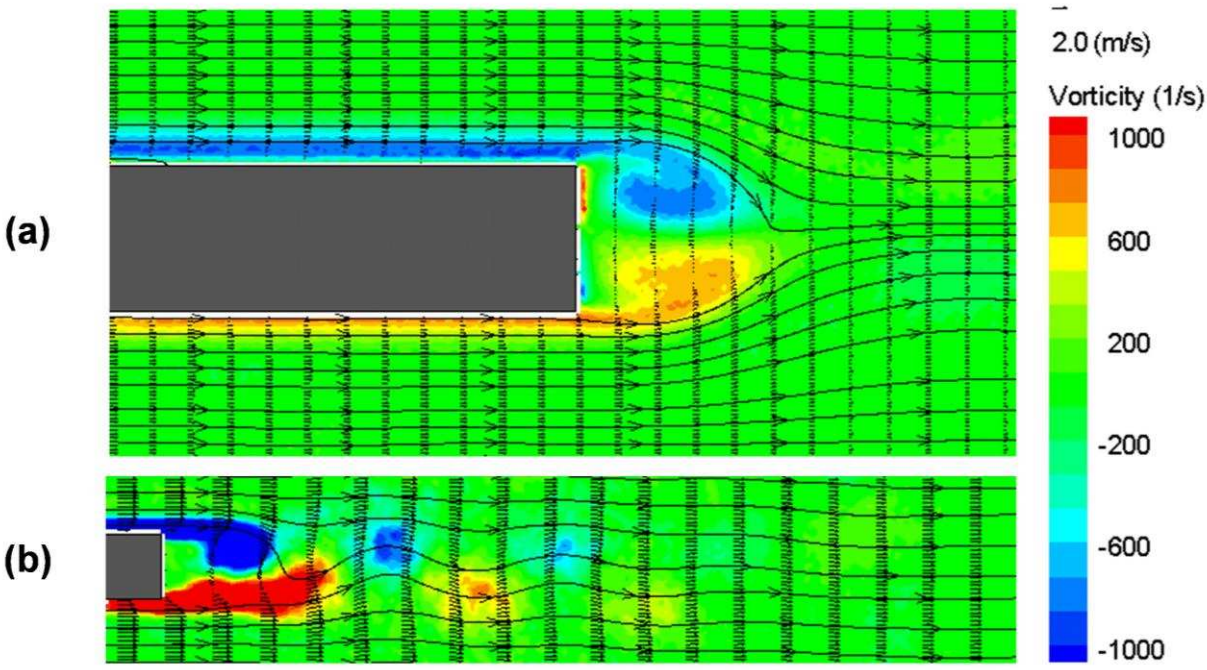

Figure 9 Mean velocity field (black arrows) superimposed on the vorticity field (colour contours) for phase Φ7 at (a) D_r = 0.3% (a close view) and (b) D_r = 1.5% (a zoom-out view). Stack plates are 5.0 mm thick with 10.0 mm gap between plates.

For the case of 5 mm thick plates, the evolution of coherent structures forming due to the separation processes is somewhat different in qualitative terms from the case of 1.1 mm thick plates. At relatively small acoustic excitation levels (e.g. D_r = 0.3%, as shown in Figure 9a), the vortex structures formed at the end of each plate are a pair of concentrated eddies that are symmetrical about the centreline of the plate. The length of these symmetrical vortex structures at the plate end is quite short compared to the plate thickness, unlike the very elongated vortex structures around the thin plates of 1.1 mm thickness. When the oscillation amplitude of the flow around the plate stack increases (e.g. D_r = 1.0%, as shown in Figure 9b), the shear layers start to roll up into discrete vortices in an alternate fashion, as soon as the symmetric wake is no longer maintained. The elongated vortex structures characteristic for the thin plates, and their further breaking-up into a "vortex street" is not observed here – see for example Mao et al. (2008). These distinct flow features, occurring as a consequence of having thin vs. thick plates or low vs. high drive ratios, should be reflected in the non-dimensional parameter space, as long as the right similarity parameters can be found. The following section will focus on defining suitable similarity numbers to characterise the types of flow discussed here.

4. Non-dimensional parameters controlling oscillatory flows at stack end

For a typical oscillatory fluid flow induced by a one-dimensional plane acoustic wave around a stack of evenly spaced parallel plates discussed in this paper, there are three groups of parameters that determine the flow behaviour. The first one includes the properties of the fluid, such as density, ρ and dynamic viscosity, μ. The second includes the geometry of the stack of parallel plates: the plate length, l, the plate thickness, d and the channel height between plates, h. The span-wise dimension of the stack of plates is not considered if the flow around it is treated as a two-dimensional problem. The third group should include the operating conditions of the acoustic wave such as its angular frequency, ω (= 2πf), and the local longitudinal velocity amplitude of the flow, u_a. However there are only three independent fundamental physical quantities that describe the seven parameters listed above; these are "length", "time" and "mass". Therefore, according to the Buckingham-Pi theorem, four independent non-dimensional parameter groups could determine the characteristics of the oscillatory flow around the plates. However, the stack length, l, is eliminated in the discussions to follow to simplify the analysis, on the basis that the fluid displacement is usually much smaller than the stack length and thus the number of non-dimensional parameter groups drops to three. Of course it is well known that the selection of non-dimensional parameters is non-unique and the analysis presented below will show two alternative "sets of three". A more general analysis, including for example the stack length, as well as other alternative sets of three non-dimensional parameters are possible based on the analogous procedures to those described.

4.1. Normalisation

It is assumed that the fluid is incompressible (which is valid only when the amplitude of the acoustic pressure oscillation is small) and that it has a constant viscosity, μ. The viscous force due to the fluid expansion can be ignored. The motion of a Newtonian fluid can be described by the Navier–Stokes equations, which in a simplified differential form can be written as

$$\begin{aligned}
\frac{\partial u}{\partial t}+u\frac{\partial u}{\partial x}+v\frac{\partial u}{\partial y}+\frac{1}{\rho}\frac{\partial p}{\partial x}&=\frac{\mu}{\rho}\left(\frac{\partial^2 u}{\partial x^2}+\frac{\partial^2 u}{\partial y^2}\right)\\
\frac{\partial v}{\partial t}+u\frac{\partial v}{\partial x}+v\frac{\partial v}{\partial y}+\frac{1}{\rho}\frac{\partial p}{\partial y}&=\frac{\mu}{\rho}\left(\frac{\partial^2 v}{\partial x^2}+\frac{\partial^2 v}{\partial y^2}\right)
\end{aligned} \qquad (2)$$

when the body forces (e.g. gravity) on unit mass of fluid can be neglected.

As mentioned above, the plate length, l, is assumed large enough for the flow disturbance caused by one end of the plate not to have an effect on the flow at the other end of the plate. The amplitude of the velocity oscillation at the stack position in an empty resonator, u_a, the plate thickness, d, and the inverse of the angular frequency of the acoustic oscillation, $1/\omega$ are chosen as the characteristic scales of velocity, length and time respectively. $\rho c u_a$ is chosen as the characteristic scale of pressure, ρc being the characteristic impedance of the fluid and c the speed of sound. The non-dimensional variables can then be written accordingly as

$$u^* = \frac{u}{u_a},\ v^* = \frac{v}{u_a\, d/h},\ x^* = \frac{x}{d},\ y^* = \frac{y}{d},\ t^* = \omega t,\ p^* = \frac{p}{\rho c u_a} \tag{3}$$

The superscript * denotes a non-dimensional variable. Of course, these are arbitrary choices of characteristic scales; other alternative approaches are possible.

The "thermodynamic" pressure p in Eq. (2) can be considered as a sum of three parts: the static pressure (or the mean pressure), the acoustic pressure originating from the propagation of the acoustic oscillation, and the dynamic pressure. The mean pressure in a thermoacoustic system is not dependent on either x or y in the resonator, so its spatial gradient is zero. The acoustic pressure is much larger than the dynamic pressure in a typical acoustic field where the particle velocity is much smaller than the sound speed ($u_a << c$). Therefore, $\rho c u_a$ is chosen as the pressure reference scale in this case.

Substituting Eq. (3) into Eq. (2), the normalized momentum equation can be written as follows

$$\begin{aligned} &\mathrm{Re}_\omega \frac{\partial u^*}{\partial t^*} + \mathrm{Re}_d \left(u^* \frac{\partial u^*}{\partial x^*} + \frac{d}{h} v^* \frac{\partial u^*}{\partial y^*} \right) + \frac{\mathrm{Re}_d}{\mathrm{Ma}} \frac{\partial p^*}{\partial x^*} = \frac{\partial^2 u^*}{\partial x^{*2}} + \frac{\partial^2 u^*}{\partial y^{*2}} \\ &\mathrm{Re}_\omega \frac{\partial v^*}{\partial t^*} + \mathrm{Re}_d \left(u^* \frac{\partial v^*}{\partial x^*} + \frac{d}{h} v^* \frac{\partial v^*}{\partial y^*} \right) + \frac{\mathrm{Re}_d}{\mathrm{Ma}} \frac{h}{d} \frac{\partial p^*}{\partial y^*} = \frac{\partial^2 v^*}{\partial x^{*2}} + \frac{\partial^2 v^*}{\partial y^{*2}} \end{aligned} \tag{4}$$

In the above equations, four non-dimensional parameter groups are defined. $\mathrm{Re}_\omega = \omega d^2/\nu$ is defined as the kinematic Reynolds number, following Worlikar and Knio (1996). It is also sometimes referred to as the Valensi number (Richardson, 1963 and Choi et al., 2004), or the non-dimensional frequency parameter (Berger and Wille, 1972). In thermoacoustics, the viscous penetration depth, δ_v, is often used as an alternative indication of the acoustic oscillation frequency. Therefore, the kinematic Reynolds number can be rewritten as $\mathrm{Re}_\omega = 2(d/\delta_v)^2$: a ratio of the plate thickness to the viscous penetration depth. The conventional Reynolds number, $\mathrm{Re}_d = u_a d/\nu$ is simply defined based on the amplitude of velocity oscillation, u_a, and the plate thickness, d.

The third non-dimensional parameter, d/h, the ratio of the plate thickness to the channel height, takes into account the effect of the existence of neighbouring plates in the stack. The channel height has an effect on the flow in two respects. Firstly, the blockage effect of the plates on the flow in the resonator has to be considered when the plate thickness is comparable with the channel height. The velocity amplitudes inside the stack differ significantly from the velocity in the empty resonator, u_a due to the blockage effect. d/h is equivalent to $1/\phi$-1, ϕ being the porosity of the stack that is defined as $\phi = h/(h+d)$ when the plates are arranged evenly. Secondly, the flow behaviour inside each channel has to be considered when the channel height, h is comparable to the thickness of the viscous boundary layer. It is clearly demonstrated that the oscillatory flow in a circular pipe remains laminar if the internal diameter of the pipe is less than approximately ten times the viscous penetration depth until the Reynolds number based on the internal diameter is over 1000 (Ohmi and Iguchi, 1982).

Although it may appear form equation (4) that the acoustic Mach number ($\mathrm{Ma} = u_a/c$) defined as the ratio of the local acoustic velocity amplitude to the sound speed is a fourth non-dimensional parameter, in reality c being constant and the flow being assumed incompressible, it has merely a meaning of velocity amplitude. It is often much smaller than unity in an acoustic field encountered in thermoacoustic applications. With the assumption of an incompressible flow, the ratio $\mathrm{Re}_d/\mathrm{Ma}$ is in effect a constant.

The amplitude of the acoustic oscillation may also be indicated by the displacement amplitude, $\xi_a = u_a/\omega$. The Keulegan-Carpenter number, KC ($= \xi_a/d$), defined as the ratio of the acoustic displacement amplitude to the plate thickness, can be introduced to indicate the flow oscillation amplitude. It is often used to describe the flow characteristics, drag/lift force or pressure distribution in the problems of bluff bodies at rest in oscillatory flow, or oscillating bluff bodies in quiescent fluid (Bearman and Graham 1980, Guilmineau and Queutey 2002), where KC is

defined as u_a/fd, a ratio of the flow orbit to a body characteristic length, with f being the frequency of flow oscillation. For a circular cylinder in an oscillating flow, the oscillating flow can be classified into different flow regimes, such as the flow that remains attached and symmetrical, the separating flow which remains symmetrical, asymmetric shedding of vortices and so forth, depending mainly on KC and weakly on the Reynolds number Re_d (Guilmineau and Queutey, 2002).

It is worth noting that another non-dimension number, the Strouhal number ($St = fd/u_a$) could be used, in the place of KC, to describe the oscillating flow characteristics (this is effectively the inverse of KC). It should be noted that f is the frequency of the acoustic oscillation (i.e. oscillatory flow forcing), not the frequency of the vortex shedding often investigated in steady flows past bluff bodies. This "forcing" Strouhal number has already been used such as in the study of the oscillatory flow around a circular cylinder (Badr et al., 1995).

The Reynolds number, Re_d can then be expressed as the product of KC number and the kinematic Reynolds number, $Re_d = KC \cdot Re_\omega$. Accordingly, equation (4) can be re-written as

$$\begin{aligned}
&\frac{\partial u^*}{\partial t^*} + KC\left(u^*\frac{\partial u^*}{\partial x^*} + \frac{d}{h}v^*\frac{\partial u^*}{\partial y^*}\right) + \frac{KC}{Ma}\frac{\partial p^*}{\partial x^*} = \frac{1}{Re_\omega}\left(\frac{\partial^2 u^*}{\partial x^{*2}} + \frac{\partial^2 u^*}{\partial y^{*2}}\right) \\
&\frac{\partial v^*}{\partial t^*} + KC\left(u^*\frac{\partial v^*}{\partial x^*} + \frac{d}{h}v^*\frac{\partial v^*}{\partial y^*}\right) + \frac{KC}{Ma}\frac{h}{d}\frac{\partial p^*}{\partial y^*} = \frac{1}{Re_\omega}\left(\frac{\partial^2 v^*}{\partial x^{*2}} + \frac{\partial^2 v^*}{\partial y^{*2}}\right)
\end{aligned} \tag{5}$$

It is clear that out of the three non-dimensional numbers, Re_d, Re_ω and KC, only two are independent, one of which could include the frequency, ω and the other the amplitude of the acoustic oscillation, either u_a or ξ_a. Equations (4) and (5) reveal that for a given non-dimensional oscillation amplitude of the flow (Re_d or KC), the relative importance of the unsteady acceleration term and the viscous term in an oscillatory flow, could be loosely described by the kinematic Reynolds number, Re_ω. Similarly, for a given kinematic Reynolds number, Re_ω, the Reynolds number, Re_d describes the relative importance of the contributions from the convective acceleration term and the viscous term, and the Keulegan-Carpenter number, KC describes the relative importance of the contributions from the unsteady acceleration term, compared with the convective acceleration term. The four force terms in Eq. (4) or (5) clearly indicate that an individual non-dimensional number could not fully describe the equilibrium of the forces. In general, if $Re_\omega >> 1$, meaning the unsteady acceleration term is much larger than the viscous term, the effect of the viscosity on the oscillatory flow will be limited to a thinner viscous boundary layer around the solid. This is also indicated by the definition of Re_ω as $2(d/\delta_v)^2$ – for a given plate thickness d, a larger Re_ω gives smaller δ_v, the viscous penetration depth. For a flow having a large Re_d (>>1), the convective acceleration term become larger than the viscous term, which could indicate that the flow being unsteady may undergo a transition to turbulence. KC, considered as the ratio of the flow displacement amplitude to the characteristic length scale (e.g. the plate thickness), could also be considered as $u_a/\omega d$. For KC>>1 the flow displacement amplitude is much greater than the plate thickness. In other words, the flow velocity amplitude is much greater or the frequency of the flow oscillation is much smaller for a given plate thickness. The effect of having KC >> 1 is to make the unsteady acceleration term much smaller than the convective acceleration term, and the behaviour of the oscillatory flow around the bluff bodies becomes less affected by the unsteady acceleration and in any instant of the oscillation the oscillatory flow acts more like a unidirectional steady flow (as if the unsteady acceleration term was dropped).

In summary, for the oscillatory flow induced by a one-dimensional plane acoustic wave around a stack of parallel plates, it involves density, ρ and dynamic viscosity, μ of the fluid, the geometry of the stack described by l, d, and h and the operating condition, u_a and the frequency. When the fluid is considered incompressible, isothermal and having a constant viscosity, the similarity of the fluid mechanics around a series of parallel plates in an acoustic field could be evaluated by the non-dimensional parameters groups (Re_ω, Re_d and d/h) or (Re_ω, KC and d/h), when the plate length is considered to be large enough.

4.2. Illustration of non-dimensional parameters concept through experimental results

Following the choice of the non-dimensional parameters to describe the behaviour of the oscillatory flow around the end of the stack of plates, the operating conditions of the oscillatory flow in the present study are shown using (Re_ω versus Re_d) and (Re_ω versus KC) planes, as illustrated in Figure 10. Also shown are the data points collected from the work conducted numerically by Worlikar and Knio (1996) and experimentally by Shi et al. (2009). The porosity, ϕ of the stacks studied is between 0.5 and 0.8, and d/h is between 0.25 and 0.5.

By visually inspecting the available data related to the development of the wake flow around the end of the stack, in particular with regard to the flow features presented and discussed in previous sections, it is possible to divide either of the two spaces, (Re_ω and Re_d) or (Re_ω and KC), into several characteristic regions. This is illustrated by the dashed lines drawn in Figure 10. These separate regions are characterised by different behaviour of the wake flow as discussed later in this section. Both the oblique and vertical dashed lines are simple straight lines in the log-log (Re_ω vs. Re_d) and (Re_ω vs. KC) planes. The oblique line can be expressed as $Re_d = 44.0Re_\omega^{0.538}$ in (Re_ω vs. Re_d) plane and $KC = 44.0Re_\omega^{0.438}$ in (Re_ω vs. KC) plane. The vertical line corresponds to $Re_\omega = 8$, when the plate thickness is equivalent to $2\delta_v$. However, clearly the dashed lines indicating the "transitions" of the flow patterns between these regions can only be sketched approximately (similar procedures are well known in defining "transitions" in multiphase flows).

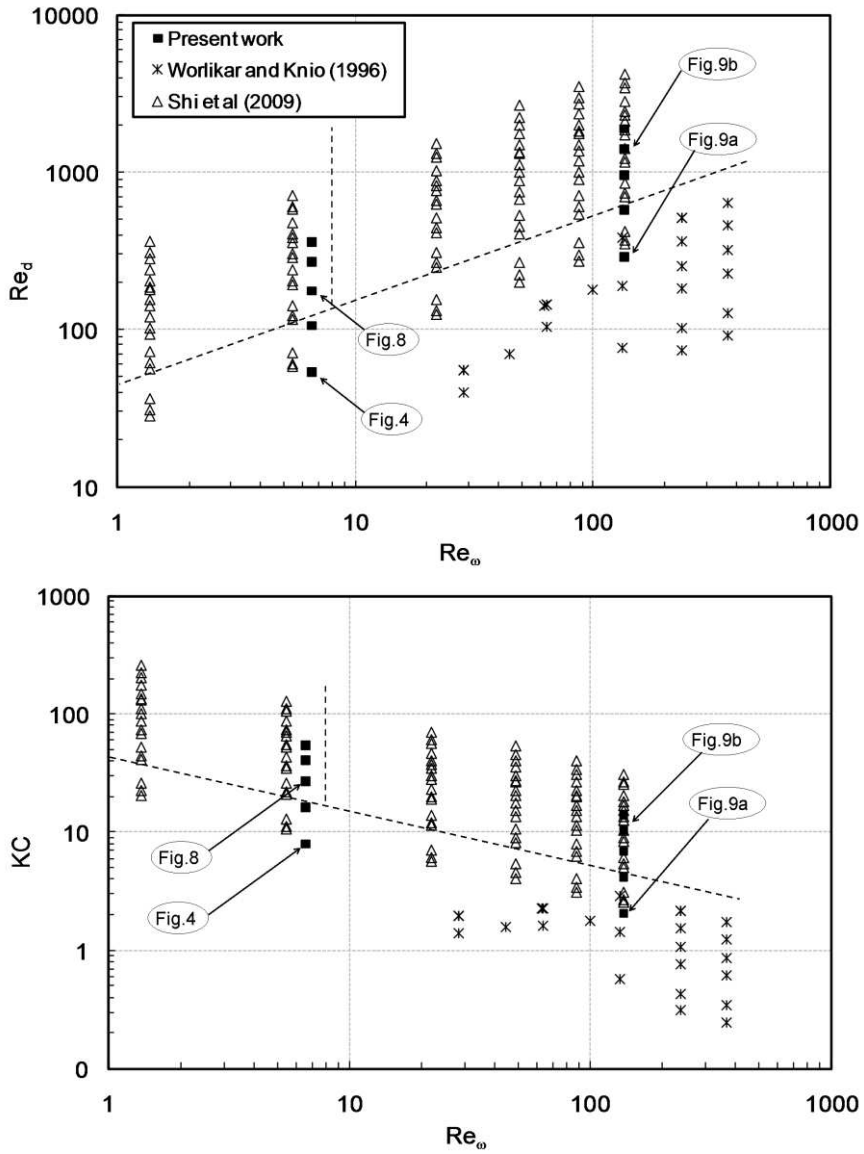

Figure 10 Operating conditions of oscillatory flow around stack of plates in non-dimensional parameter groups (Re_ω vs. Re_d) and (Re_ω vs. KC)

In general, the state of the flow below the dashed oblique line is often symmetric about the plate centreline, even though the symmetric vortex structure may have a larger longitudinal length compared with the plate thickness when Re_ω is smaller than 8, while the vortex structure often takes the form of much concentrated eddies when Re_ω is larger than 8. On the other hand, the flow behind the end of the plates in the region above this line is often asymmetric. Complicated flow patterns, such as the shear layers in the wake breaking up into "vortex street" type structure or the shear layers rolling up into vortices and shedding in an alternate fashion, may start to appear.

The region above the dashed oblique line can be further separated into two sub-regions by the vertical dashed line. The flow in the conditions that fall into the left region can often develop into an elongated shear layer structures in the end of the plate. Then this elongated shear layer becomes asymmetric possibly due to the instability of the shear layers, and eventually breaks up into discrete vortices. On the right hand side of the vertical dashed line, the flow at the end of the plate often exhibits vortex shedding before the elongated shear layer structure can be formed, and leads to a pattern similar to the von Karman vortex street. However, admittedly the flow in both regions could develop into much more complicated flow patterns when Re_d or KC increase further, as shown by Shi et al. (2009).

The flow conditions of the four cases discussed in Section 3 are indicated by the arrows in Figure 10. The flow pattern of each of these two cases below the oblique line (i.e. Fig.4 and Fig.9a) clearly represents the state of the flow behind the plate stack. It is interesting to see that the flow conditions that all fall into the same region as that for Fig.9a are collected from the numerical work by Worlikar and Knio (1996), who adopted similar geometrical configurations of plate stacks to that used by Atchley et al. (1990) in an experimental study of acoustically generated temperature gradient due to thermoacoustic effect. The behaviour of the flow in each sub-region above the oblique line can be illustrated by Fig.8 and Fig.9b when the values of Re_d and KC are not too far from the line.

The presence of the neighbouring plates around the plate studied could have an effect on the gradient of the velocity profile in the shear layer wake and thus the ability of the wake flow to remain symmetric. However, it is still rather difficult at this stage to identify the effect of the channel width on the flow based on the available experimental and numerical data. Therefore the effect of the non-dimensional number, d/h or the porosity, ϕ, on the flow behaviour is not distinguishable in these graphs.

5. Discussion and conclusion

This paper investigates the behaviour of the oscillatory flow past a stack of parallel plates when the fluid moves out of the stack (so-called "ejection stage" of the cycle). It can be seen that during this part of the acoustic cycle the flow exhibits some similarities to the wake flow of a unidirectional steady flow past a bluff body, such as a circular cylinder (Zdravkovich, 1997). Essentially, the wake flow is made up of two shear layers with vorticity of opposite signs that are fed from the stack channel. There may be a recirculation region formed next to the plate end, and surrounded by the shear layers. The size of the recirculation region increases while the flow speeds up in the initial stage of the "ejection"; then continues to grow even in the deceleration phases of the "ejecting" flow. The flow in the recirculation region finally joins with the flow that reverses its direction and starts to move into the stack.

The oscillating flow at the end of plate also shows interesting behaviour when the velocity amplitude varies. At small amplitudes the shear layers in the wake may remain symmetric and produce attached symmetrical vortex structures. However for larger velocity amplitudes the flow may lose its symmetry and stability, resulting in such flow patterns as "break-up" of the shear layers and alternate vortex shedding. It is shown that the break-up of the shear layers may undergo a transition to the alternate shedding, however the alternate shedding may also start in the first place without such a transition taking place. It seems plausible that both the lateral and longitudinal dimensions of the shear layers in the wake define the flow patterns and their development.

From the normalization of the governing equations of the oscillatory flow motion around a parallel plate, groups of non-dimensional parameters are proposed. Each set of non-dimensional parameters essentially consists of: (i) one kinematic parameter, i.e. the kinematic Reynolds number Re_ω, (ii) one dynamic parameter, i.e. the Reynolds number Re_d or KC, or

more indirectly the drive ratio, Dr, and (iii) a stack configuration parameter, d/h, or the porosity ϕ. Alternatively, the Womersley number (Womersley 1955), Wo = h/δ_v could be used as the stack configuration parameter, for it is simply equivalent to h/d(Re_d/2KC)$^{1/2}$. As indicated in Eq. (1), Wo number could be used to describe the interaction of the viscous boundary layers on the neighbouring plates. Therefore, the non-dimensional parameters groups (Re_ω, Re_d and Wo) or (Re_ω, KC and Wo) could be used in place of the non-dimensional parameters groups (Re_ω, Re_d and d/h) or (Re_ω, KC and d/h).

An additional parameter – the non-dimensional stack length, i.e. the aspect ratio l/d, may need to be considered when the displacement amplitude of the fluid oscillation is comparable to the stack length so that the assumption that the flow disturbance at one end of the stack has no effect on the flow at the other end of the stack is no longer valid. Figure 10 demonstrates how the data collected from the current study and the data from other studies that can be found in the existing literature can be gathered in a single plot and divided into regions of distinct flow behaviour – in a similar way as known flow regime maps in other areas of fluid mechanics.

In order to further understand the relationship between the non-dimensional governing parameters and the flow behaviour, experimental data from much more diverse experimental conditions than these obtained as part of the current study will be required. In particular, the critical values of the non-dimensional parameters, which correspond to the transition from symmetric to asymmetric wake flows, need to be studied. Similarly, the effects of the channel width on the flow pattern should be investigated.

References:

1. Aben P C H, Bloemen P R and Zeegers J C H, 2009, 2-D PIV measurements of oscillatory flow around parallel plates, Experiments in Fluids, 46, 631–641
2. Arnott W. P., Bass H. E., and Raspet R., 1991, General formulation of thermoacoustics for stacks having arbitrarily shaped pore cross sections, Journal of the Acoustical Society of America, 90, 3228-3237
3. Atchley A. A., Hofler T. J., Muzzerall M. L., Kite M. D., and Ao C., 1990, Acoustically generated temperature gradients in short plates, Journal of the Acoustical Society of America, 88, 251-263
4. Backhaus S., Swift G. W., 2001, Fabrication and use of parallel plate regenerators in thermoacoustic engines, Proceedings of 36th Intersociety Energy Conversion Engineering Conference (IECEC), eds. Somasundaram S, Allen D H et al, vol 1 pp. 453-458 (New York: ASME)
5. Badr, H. M., Dennis, S. C. R., Kocabiyik, S. and Nguyen, P., 1995, Viscous oscillatory flow about a circular cylinder at small to moderate Strouhal number, Journal of Fluid Mechanics, 303, 215-232
6. Bearman P. W., Graham J. M. R., 1980, Vortex shedding from bluff bodies in oscillatory flow: A report on Euromech 119, Journal of Fluid Mechanics, 99, 225-245
7. Bearman P. W., 1984, Vortex shedding from oscillating bluff bodies, Annual Review of Fluid Mechanics, 16, 195-222
8. Berger E., Wille R., 1972, Periodic flow phenomena, Annual Review of Fluid Mechanics, 4, 313-340
9. Choi S., Nam K., Jeong S., 2004, Investigation on the pressure drop characteristics of cryocooler regenerators under oscillating flow and pulsating pressure conditions, Cryogenics, 44, 203-210
10. Guilmineau, E., and Queutey, P., 2002, A numerical simulation of vortex shedding from an oscillating circular cylinder, Journal of Fluids and Structures, 16(6), 773-794
11. Hofler T. J., 1986, Thermoacoustic refrigerator design and performance, PhD thesis, Physics department, University of California, San Diego
12. Kovasznay L. S. G., 1949, Hot-Wire Investigation of the Wake behind Cylinders at Low Reynolds Numbers, Proceedings of the Royal Society of London. Series A, Mathematical and Physical Sciences, 198(1053), 174-190
13. Mao X., Marx D., Jaworski A. J., 2005, PIV measurement of coherent structures and turbulence created by an oscillating flow at the end of a thermoacoustic stack, Progress in Turbulence II, Proc. of the iTi Conference in Turbulence 2005 (Springer Proceedings in Physics vol. 109 2007) eds. Oberlack M, Khujadze G et al (Berlin: Springer) pp. 99-102
14. Mao X., Yu Z., Jaworski A. J., and Marx D., 2008, PIV studies of coherent structures generated at the end of a stack of parallel plates in a standing wave acoustic field, Experiments in Fluids, 45, 833-846

15. Marx D, Mao X and Jaworski A J, 2006, Acoustic coupling between the loudspeaker and the resonator in a standing-wave thermoacoustic device, Applied Acoustics, 67, 402–419
16. Ohmi, M. and Iguchi, M., 1982, Critical Reynolds number in an oscillating pipe flow, Bulletin of JSME, 25(200), 165-172
17. Paek I., Braun J. E., Mongeau L., 2005, Second law performance of thermoacoustic systems, Journal of the Acoustical Society of America, 118, 1892
18. Rayleigh J. W., The Theory of Sound, 1894. Dover Publications, New York, 1945
19. Richardson P. D., 1963, Note: Comments on viscous damping in oscillating liquid columns, International Journal of Mechanical Sciences, 5(5), 415-418
20. Rott N., 1980, Thermoacoustics, Advances in Applied Mechanics, 20, 135-175
21. Shi L., Yu Z., Jaworski A. J., 2009, Vortex formation at the end of the parallel-plate stack in the standing-wave thermoacoustic device, Proceedings of The Sixteenth International Congress on Sound and Vibration, Kraków, Poland, 5-9 July 2009.
22. Swift G. W., 1988, Thermoacoustic engines, Journal of the Acoustical Society of America, 84(4), 1145-1180
23. Swift G. W., 2001, Thermoacoustics: A unifying perspective for some engines and refrigerators, Acoustical Society of America.
24. Womersley J. R., 1955, Method for the calculation of velocity, rate of flow and viscous drag in arteries when the pressure gradient is known, Journal of Physiology, 127, 553-563
25. Worlikar A. S., Knio O. M., Klein R., 1996, Numerical simulation of a thermoacoustic refrigerator, Proceedings of ESAIM, Vol. 1, 363-375
26. Worlikar A. S., Knio O. M., 1996, Numerical simulation of a thermoacoustic refrigerator I: Unsteady adiabatic flow around the stack, Journal of Computational Physics, 127, 424-451
27. Zdravkovich M. M., 1997, Flow around circular cylinders, Volume 1: Fundamentals, Oxford University Press